Energetics and structure of single Ti defects and their influence on the decomposition of $NaAlH_4$

Cunke Huang,[ac] Yu-Jun Zhao,[b] Hui Wang,[a] Jin Guo[c] and Min Zhu*[a]

Received 17th April 2010, Accepted 20th September 2010
DOI: 10.1039/c0cp00255k

The energetics and structure of various types of single extrinsic Ti defects in $NaAlH_4$ bulk and (001) slab at the hydriding/dehydriding critical point environment were studied systematically. It is found that the most favorable situation is Ti substituting Al at the subsurface (Ti_{Al}(2nd)), which has the highest coordination number for extrinsic Ti ions. The most stable Ti defect in the 1st layer is located at the Al rich interstitial site, namely Ti_i(1st), accompanied with remarkable strength of Ti–H/Al bond and local geometry deformation at the 1st layer around Ti. Deeper insight of the formation mechanism of Ti defects is obtained by dividing the formation enthalpy of Ti defects into three terms, which are contributed from the cost of removing a substituted host atom if necessary, the cost of structure deformation, and the gain of bonding between Ti and its surrounding ions in the formation of the defects. This associates the formation energy directly with the local structure of Ti defects. For the first time, we adopt H_f(H), H_f(H–H), H_f(AlH_3) and H_f(Na) to discuss the hydrogen release ability of the Ti doped $NaAlH_4$. We find that $TiAl_4H_{20}$ and $TiAl_3H_{12}$ complexes are formed around Ti_{Al}(2nd) and Ti_i(1st) respectively, which significantly promotes the dehydriding ability of $NaAlH_4$. What is more, the catalyst mechanism of Ti on the decomposition of $NaAlH_4$ is linked to the AlH_3 mechanism according to our calculations.

1. Introduction

Since the discovery that hydriding/dehydriding reversibility and the reaction kinetics of $NaAlH_4$ can be greatly improved by doping with Ti-containing catalysts,[1] alanates, amides and borohydrides have become a focus in hydrogen storage materials researches.[2–4] Although the importance of Ti-containing catalysts is well recognized, the catalytic mechanism is not well understood.

It is challenging to determine the location and local structure as well as the influence of extrinsic Ti defects in experiments at the atomic level, especially for the materials involving hydrogen atoms. Meanwhile, computational methods are advantageous for these studies of well-defined model systems. Ke *et al.*[5] have done an outstanding work on the decomposition reactions of $NaAlH_4$, Na_3AlH_6 and NaH with first-principles method, and they strongly suggested further investigation on the doped $NaAlH_4$ system.

Many first-principles studies have been attributed to the catalytic mechanism of Ti defects. Iniguez *et al.*[6,7] reported that Ti prefers to substitute Na in the bulk or surface of $NaAlH_4$ and it would shorten the distance of H–H and facilitate the formation and release of H_2. There are also some reports[8–10] that Ti is favorable to substitute Al in bulk of $NaAlH_4$, and the corresponding improvement in hydriding/dehydriding behavior is attributed to the formation of Ti–Al bonds, which weaken Al–H bonds nearby. Liu *et al.*[11–13] showed that Ti is favorable at interstitial sites at the surface and forms $TiAl_3H_{12}$ complexes, which may be a precursor of $TiAl_3$. They suggested that the hydrogen desorption energy is thus considerably smaller than that from a clean $NaAlH_4$ surface. In addition, Marashdeh *et al.*[14] showed that Ti is more stable at the subsurface of the $NaAlH_4$ than on the surface, and prefers to substitute Na ions. They also suggested a zipper mechanism for hydriding of $NaAlH_4$. Vegge[15] reported that Ti_{Na}–$2V_{Na}$ on the surface of $NaAlH_4$ can lower the barriers for H_2 desorption about 1 eV. Gunaydin *et al.*[16] suggested that the Ti dopant can assist breaking the H–AlH_3 bonds and that AlH_3 vacancies play an important role in the decomposition of $NaAlH_4$, though they did not give the detailed location of the extrinsic Ti defects.

Generally, Ti defects with higher formation enthalpy have higher activity, so they also have more remarkable effect on the hydriding/dehydriding performance when present. That is why various kinds of Ti defects can improve the hydriding/dehydriding performance of $NaAlH_4$ as reported in the above literature results. However, it is obvious that the extrinsic Ti defects with high formation enthalpy have low possibility to form. Therefore, it is necessary to study the detailed energetics and structure of extrinsic Ti defects in order to get an insight of its catalyst mechanism.[5]

In this paper, a first-principles method is adopted to study the extrinsic Ti defects in $NaAlH_4$ systematically. First, we compare as many as possible types of Ti defects (*cf.* section 3.1). Second, we consider the chemical environment for the formation of Ti defects. The defects introduced in the samples are uniquely

[a] *School of Materials Science and Engineering, South China University of Technology, Guangzhou 510640, P. R. China. E-mail: hckxy@yahoo.cn, memzhu@scut.edu.cn; Fax: (+86) 020-87111317; Tel: (+86) 020-87113924*
[b] *Department of Physics, South China University of Technology, Guangzhou 510640, P. R. China. E-mail: zhaoyj@scut.edu.cn, mehwang@scut.edu.cn*
[c] *College of Physics Science and Technology, Guangxi University, Nanning 530004, P. R. China. E-mail: guojin@gxu.edu.cn*

determined by the practical hydriding/dehydriding chemical environment, which can be described by the chemical potentials of components. Therefore, the Ti defects are studied at the chemical environment corresponding to the hydriding/dehydriding critical point[17] (*cf.* section 3.1). Third, the most stable charge state of the extrinsic Ti defects is investigated according to charge neutrality of the Ti doped $NaAlH_4$ system including as many as possible intrinsic and extrinsic defects. At the balanced Fermi level, we find that the neutral state reflects the most stable charge state of the most crucial extrinsic Ti defects, such as Ti_{Al}(2nd), in the Ti-doped $NaAlH_4$ at the critical hydriding/dehydriding point. Furthermore, we divide the formation enthalpies of Ti defects into several components based on a virtual process of the defect formation. All of these components have physical meaning and are corresponding to the local structure of the Ti defects. In this way, more details of formation mechanism of the most stable Ti defects can be understood.

Based on the determined favorable location of Ti defects, we further study the energetics of Ti defects with respect to its local structures, which is helpful to understand the influence of Ti on the initial stage of the decomposition of $NaAlH_4$ with assistance from Ti defects.

2. Computational methods

We performed DFT plane-wave calculations of a Ti-doped $NaAlH_4$ 2 × 2 × 2 supercell (16 $NaAlH_4$ units) and a 2 × 2 (001) slab (7 layers of Na/Al cations, 28 $NaAlH_4$ units) using the VASP code.[18,19] The (001) surface is a close packed surface with the lowest surface energy.[15] A vacuum space of 15 Å along the *z* directions is employed to simulate the surface. The Al and Na ions in the two bottom layers of the slab were fixed during relaxation, while all the H ions are relaxed in order to diminish the influence of surface polarization.[12] The Projector Augmented Wave (PAW) potential was used to describe electron–ion interactions and the PW91 GGA approximation[20] was employed to calculate exchange and correlation energy. The Brillouin zone was generated by the Monkhorst–Pack scheme with 5 × 5 × 3 for the supercell and 5 × 5 × 1 for the slab. The cut-off energy for plane waves was 500 eV.

3. Results and discussion

3.1 The formation enthalpies of extrinsic Ti defects

The formation enthalpies of defect were calculated from eqn (1):[21]

$$H_f(\text{def}) = E(\text{def}) - E(\text{bulk/slab}) - \sum_i n_i(\Delta\mu_i + \mu_i^{\text{crys}}) \quad (1)$$

Here, H_f(def) is the defect formation enthalpy; E(def) is the calculated total energy of the supercell/slab with defect; E(bulk/slab) is the calculated total energy of the supercell/slab without defect. μ_i^{crys} is the chemical potential of component i in the most stable elemental crystal which is adopted as the reference for convenience. $\Delta\mu_i$ is the relative chemical potential of component i, and $\mu_i = \Delta\mu_i + \mu_i^{\text{crys}}$ is the chemical potential of component i in the real chemical environment. n_i denotes the number of ions of species i, which is added ($n_i > 0$) or removed ($n_i < 0$) during the formation of a defect. It is obvious that the lower H_f(def) is, the more stable the extrinsic Ti defect is.

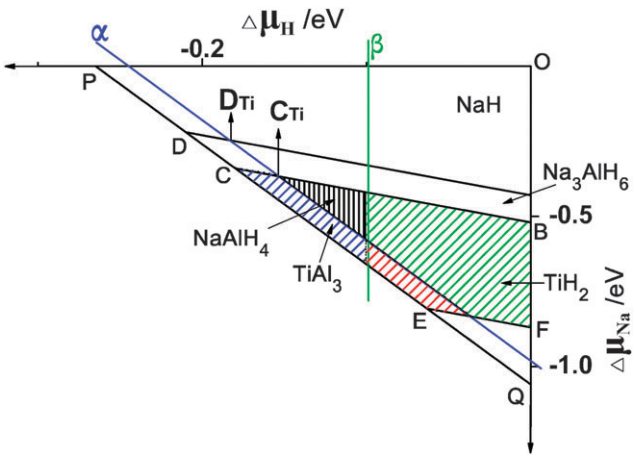

Fig. 1 The chemical potential phase diagram of Ti–$NaAlH_4$. Region BCEF and the black shadowed region corresponds to SCPR of $NaAlH_4$; and the points C and C_{Ti} are the hydriding/dehydriding critical points of $NaAlH_4$ before and after doped with Ti respectively.

The defect formation enthalpy is influenced by the chemical environment. Therefore, only when the chemical environment corresponding to the practical experimental condition is adopted, the calculated defect formation enthalpies reflect the actual defect stability. Here, the chemical environment is discussed according to the equilibrium of the Ti–Na–Al–H phase diagram (Fig. 1).

Before adding Ti dopants, lines OP, OQ and PQ correspond to the pure Na, H_2 and Al phase, respectively. Lines BC, EF correspond to the critical equilibrium line of $NaAlH_4$/Na_3AlH_6 and $NaAlH_4$/AlH_3, respectively. The trapezoid region BCEF corresponds to the stable chemical potential range (SCPR) of $NaAlH_4$. Points F, C and B correspond to the Na poorest, H poorest, and Al poorest chemical environment, respectively. Hydriding/dehydriding reaction of $NaAlH_4$ will take place when the chemical potential of H in the environment is higher/lower than that at point C. Therefore, point C is called the hydriding/dehydriding critical point of $NaAlH_4$[17]. Similarly, point D is the hydriding/dehydriding critical point of Na_3AlH_6.

As shown in ref. 17, $TiAl_3$ (blue region) and TiH_2 (green region) competing phases will form in Al rich and H rich areas when $\Delta\mu_{Ti} > -1.55$ eV, which leads to a shrinking of the SCPR of $NaAlH_4$ (black region when doped) and a shift of the hydriding/dehydriding critical point (*e.g.* from C to C_{Ti} in Fig. 1). When $\Delta\mu_{Ti} > -1.26$ eV, the SCPR of $NaAlH_4$ disappears, and thus the system can no longer undergo rehydriding. While $\Delta\mu_{Ti} \ll -1.59$ eV, the Ti-containing competing phases do not form and the concentration of Ti defects is too low to catalyse the hydriding/dehydriding in $NaAlH_4$. In practice, $\Delta\mu_{Ti}$ should be tuned to slightly greater than −1.59 eV, which is the maximum value of $\Delta\mu_{Ti}$ not affecting the SCPR of pure $NaAlH_4$. In this paper, we adopt the critical value of $\Delta\mu_{Ti} = -1.59$ eV for the analysis of the stability of Ti defects. When $\Delta\mu_{Ti} = -1.59$ eV, $\Delta\mu_{Na}$, $\Delta\mu_{Al}$ and $\Delta\mu_H$ are corresponding to the values at the critical point of

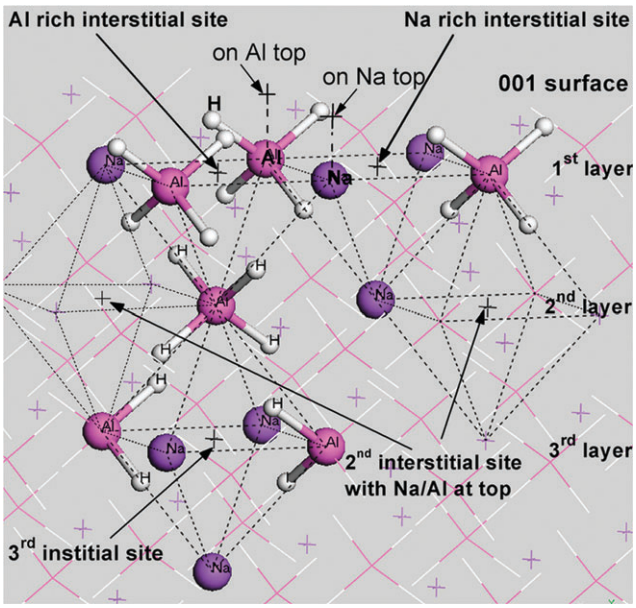

Fig. 2 The possible sites of Ti defects before structure relaxation.

$NaAlH_4$ (point C) since it is not shifted by Ti dopants. Obviously, at this chemical environment, the upper limit of the formation enthalpies of substitutional Ti defects at Al and Na sites are obtained, since $\Delta\mu_{Al}$ and $\Delta\mu_{Na}$ decrease as the hydriding/dehydriding critical point shifts upwards.

In this work, we have considered as many extrinsic Ti defects as possible. From the space aspect, we consider Ti defects located at the 1st layer, the 2nd layer, the 3rd layer as well as in the bulk of $NaAlH_4$. From the aspect of Ti defect types, we consider interstitial defects at octahedron sites, Ti substituting Na/Al, and Ti exchanging with Na/Al when Ti locates on the surface. The Na–Al bridge site at the 1st layer and tetrahedron interstitial site are not considered because the distance between Ti and its nearest neighbor (NN) ions is too short. We have also calculated other complex defects like Ti_{Na}–V_{Na} and Ti_{Na}–$2V_{Na}$. Our calculated results indicate that these defects are difficult to form and we do not discuss them in this paper. All these locations of Ti before structure relaxation are shown in Fig. 2.

It should be pointed out that the situation of Ti located at an octahedron interstitial site is more complicated than the others. There is only one type of octahedron in the bulk of $NaAlH_4$ which has three Na cations and three Al cations at its vertexes, while there are quite a few interstitial sites near the surface because the translational symmetry disappears along the direction perpendicular to the surface. At the 1st layer, the interstitial sites with 3 NN Al and 2 NN Na cations are referred to "Al-rich" interstitial sites, while "Na-rich" interstitial sites are surrounded with 2 NN Al and 3 NN Na cations (*cf.* Fig. 2). They are denoted by Ti_i(1st Al rich) and Ti_i(1st Na rich), and the former is simplified to Ti_i(1st) due to its lower formation enthalpy in the text later. Besides, we have considered Ti defects locating at the 2nd layer octahedron interstitial site with Na/Al at the top of it (*cf.* Fig. 3l and 3I).

The local structures of Ti defects after structure relaxation are shown in Fig. 3. It shows that the neighbor H and Al ions are attracted by Ti while Na cations nearby are repulsed, because Ti has good affinity with Al and H but not with Na. As a result, Ti–H_x or Ti–Al_x–H_y complex forms around Ti. There is an obvious difference between any two relaxed Ti-containing local structures of *different types*, while Ti-containing local structures with the *same type* are similar to each other except the situation of Ti at the 1st layer. Generally, the relaxed local structures of Ti-containing complexes are not similar unless the distribution of Na/Al/H ions around Ti before relaxation is similar. We highlight some ions near Ti for a better visualization. For interstitial Ti defects, we highlight the $TiAl_3H_{12}$ complex in accordance with an earlier reported structure.[11–13] For Ti substituting Na situations, the TiH_8 (TiH_6 at 1st layer) complexes were highlighted in line with the work by Løvvik *et al.*[8] As for Ti substituting Al situations, we highlight the $TiAl_4H_{20}$ ($TiAl_2H_{12}$ at 1st layer) complex in Fig. 3.

H_f(def) of the Ti defects at different depths in the (001) slab of $NaAlH_4$ are shown in Fig. 4a. It is obvious that the defect of Ti substituting Al at 2nd layer, labeled with Ti_{Al}(2nd) (Fig. 3k), is the most stable among all the Ti defects which is consistent with Løvvik *et al.*[8] Its formation enthalpy at the hydriding/dehydriding critical point is 2.01 eV. In the 1st layer, Ti is most favorable at the Al rich interstitial site, Ti_i(1st) (Fig. 3e), which is in accordance with the result in ref. 12, and its formation enthalpy $H_f(Ti_i(1st))$ is 3.08 eV at the hydriding/dehydriding critical point. In addition, from the space aspect, H_f(def) is obviously higher than others when Ti locates outside of 1st layer metal of (001) slab. From the aspect of defect type, H_f(def) of Ti exchanging with surface Na/Al and Ti on the surface are so high that they are difficult to form. Therefore, in the following, we only consider three types of extrinsic Ti defects: Ti_{Al}, Ti_{Na} and Ti_i.

Fig. 4b is plotted for a convenient comparison of the formation enthalpies of the three types of Ti defects: Ti_{Al}, Ti_{Na} and Ti_i. As shown in Fig. 4b, the stability of these Ti defects at the same layer in the sequence from high to low is $Ti_{Al} > Ti_i > Ti_{Na}$ except the Ti_i(1st). For defects of Ti substituting Na, the stability of Ti defect reduces gradually with increase of its depth in slab. For Ti_i defects at the 1st layer, the formation enthalpy in Al rich interstitial sites is much lower than that in Na rich interstitial sites, while the difference between different interstitial sites at the 2nd layer is much smaller. If only the Ti_i defects with lower formation enthalpy at a layer is considered, the stability of defect reduces gradually with its depth increasing. As for the defect of Ti substituting Al type, Ti_{Al}(2nd) is the most stable one. There are little difference for $H_f(Ti_{Al})$ in different layers except Ti_{Al}(2nd). For all types of Ti defects, the defect formation enthalpy in the 3rd layer has no remarkable difference with that in bulk.

From above results, Ti_{Al}(2nd) is obviously the most stable extrinsic Ti defect in $NaAlH_4$. However, considering that there are kinetic barriers before Ti reaches Ti_{Al}(2nd) site when it migrates from outside of $NaAlH_4$, we expect that most Ti defects may initially be formed at the 1st layer. $H_f[Ti_i(1st)]$ is the lowest among Ti defects near the 1st layer at the hydriding/dehydriding critical point, and it was studied by Liu *et al.*[11–13] Furthermore, the Ti site of Ti_i(1st) is right on the top of that of

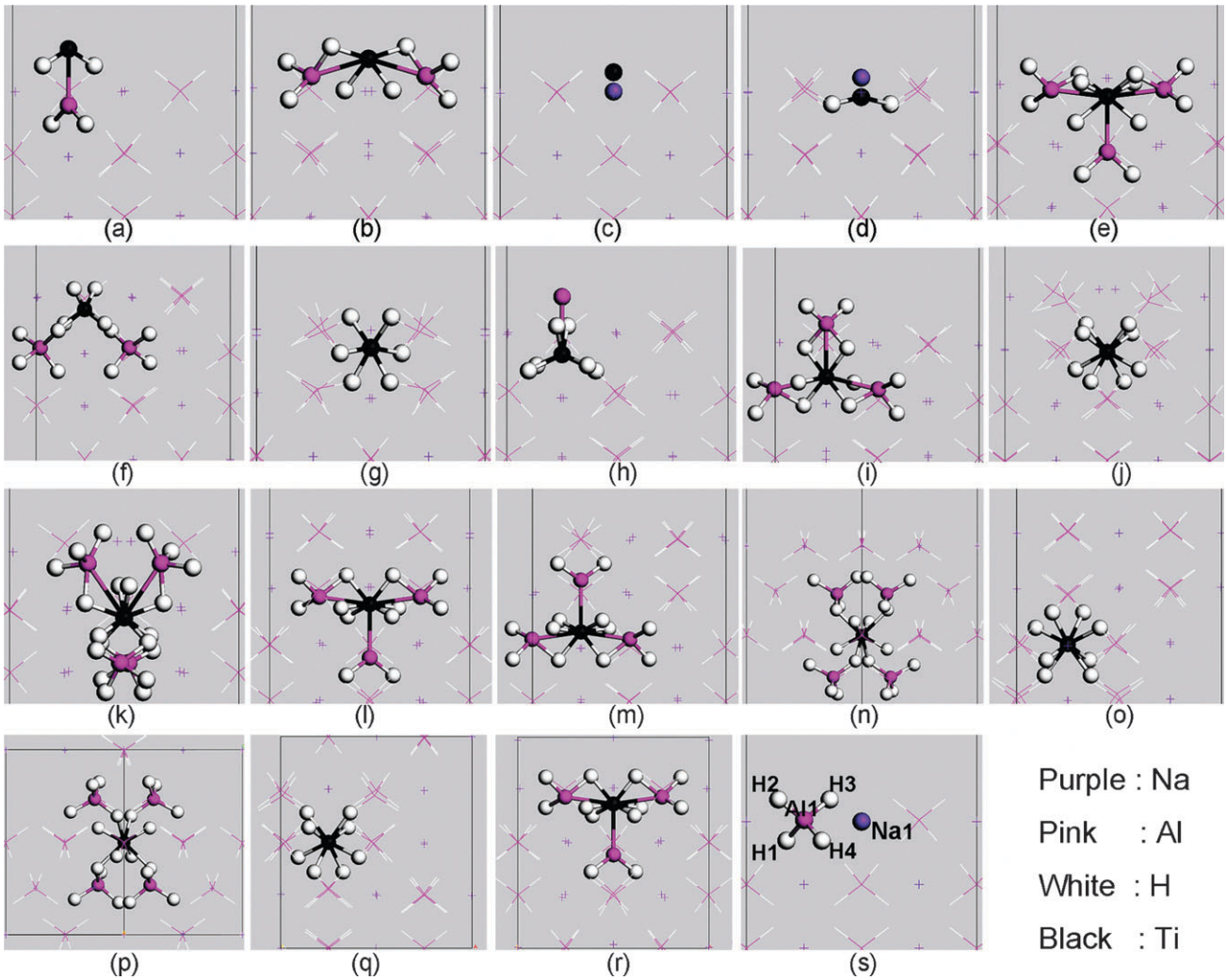

Fig. 3 Relaxed local structures of Ti-containing complexes in Ti-doping model and AlH_4 complex in clean (001) slab. (a)–(o) correspond to the Ti defect at surface, subsurface and the third layer, which are arranged by the Z coordination of Ti from large to small in the $NaAlH_4$ (001) slab. (a): Ti at Al site on surface; (b): Ti at surface Na rich interstitial site [Ti_i(1st Na rich)]; (c): Ti at Na site on surface; (d): Ti exchanging with surface Na [$Ti_{Na-NaTi}$(1st)]; (e): Ti at surface Al rich interstitial site [Ti_i(1st)]; (f): Ti substituting surface Al [Ti_{Al}(1st)]; (g): Ti substituting surface Na [Ti_{Na}(1st)]; (h): Ti exchanging with surface Al [Ti_{Al}–Al_{Ti}(1st)]; (i): Ti at 2nd layer interstitial site with Al at top [Ti_i(2nd_Al@top)]; (j): Ti substituting the 2nd layer Na [Ti_{Na}(2nd)]; (k): Ti substituting the 2nd layer Al [Ti_{Al}(2nd)]; (l): Ti at 2nd layer interstitial site with Na at top [Ti_i(2nd)]; (m): Ti at 3rd layer interstitial site [Ti_i(3rd)]; (n): Ti substituting the 3rd layer Al [Ti_{Al}(3rd)]; (o): Ti substituting the 3rd layer Na [Ti_{Na}(3rd)]; (p): Ti substituting Al in bulk [Ti_{Al}(bulk)]; (q): Ti substituting Na in bulk [Ti_{Na}(bulk)]; (r): Ti at interstitial site of bulk [Ti_i(bulk)]; (s) clean (001) slab.

Ti_{Al}(2nd), and the former defect may be a precursor of the later one. Therefore, Ti_i(1st) also plays a crucial role in the Ti catalysis for dehydrogenation. We will discuss the influence of Ti_{Al}(2nd) and Ti_i(1st) on decomposition of $NaAlH_4$ in a later section.

3.2 Decomposition of H_f(def)

Here, we decompose H_f(def) in accordance with a virtual process of the defect formation. We presume that the formation process of a Ti defect can be divided into three stages, exemplified with the Ti_{Na} defect in the following. Firstly, it costs energy of $H_f(V_{Na})$ to remove one Na atom from the bulk of $NaAlH_4$ *i.e.*, the formation of V_{Na}. Next, a Ti atom from the environment is put into the vacancy site and has its neighbor ions adjusting their position without considering the bonding between Ti and its surrounding (energetic-wise). It will cost a deformation energy, $E_d(Ti_{Na})$. Finally, Ti atom will bond with its surrounding ions with an energy gain of $E_b(Ti_{Na})$. Thus, the formation enthalpy of a Ti defect can be expressed as the sum of three terms:

$$H_f(Ti_M) = E_d(Ti_M) + H_f(V_M) - E_b(Ti_M)\ (M = Al, Na, i) \quad (2)$$

Here, "i" means "octahedral interstitial site", and obviously that $H_f(V_i) = 0$. It should be pointed out that $E_d(Ti_M)$, $E_b(Ti_M)$ and $H_f(V_M)$ have physical meanings and can be calculated by a first-principles method. Furthermore, they are closely related to the local structure of defect site which is of advantage in discussing the formation mechanism of Ti defects by combining those energies with Ti-containing local structure.

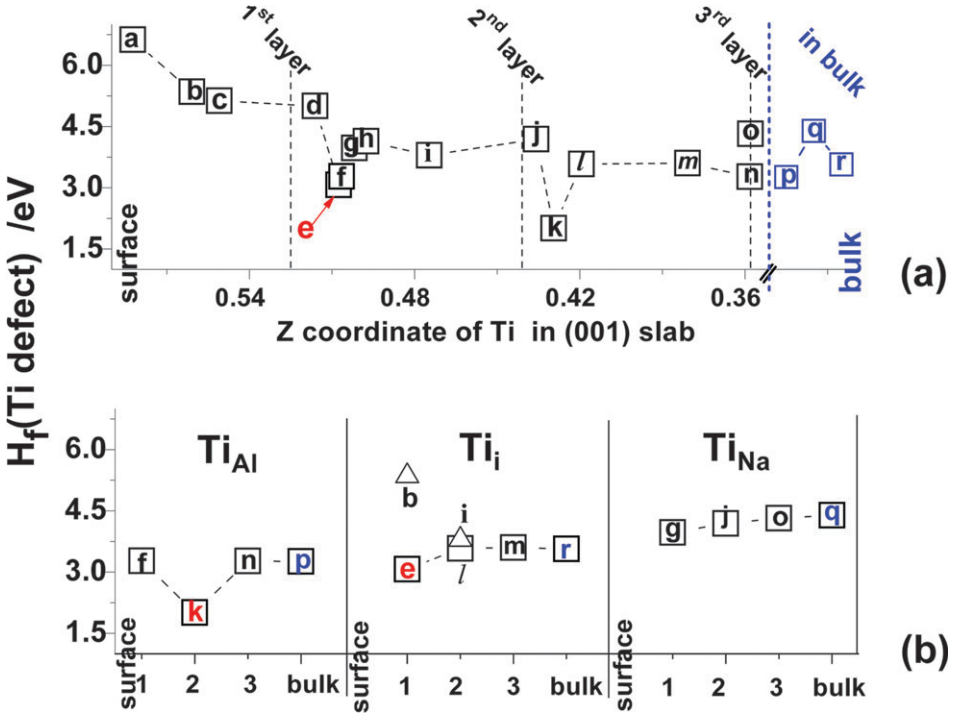

Fig. 4 (a) The relation of H_f(Ti defect) *vs.* (depth of Ti) in (001) slab of $NaAlH_4$. (b) $H_f(Ti_{Al})$, $H_f(Ti_{Na})$, $H_f(Ti_i)$ in the 1st, 2nd and 3rd layer from the surface of (001) slab and in bulk of $NaAlH_4$.

$H_f(Ti_M)$ is increased by $E_d(Ti_M)$ and reduced by $E_b(Ti_M)$, while the bonding and deformation energy induced by Ti are correlative. We know that the displacement of neighbor Al/H/Na occurs during relaxation when Ti ion bonds with its neighbor Al/H ions, which should be balanced in the end. It is easy to know that a stronger attraction between Ti and its neighbor Al/H ions needs to be balanced by a greater deformation around the Ti ion in principle. We can see later in Fig. 6 that if the configuration of Ti-containing complexes are similar, higher $E_b(Ti_M)$ corresponds to higher $E_d(Ti_M)$ and lower H_f(Ti def). Therefore, the stability of Ti defects can be described qualitatively by either the bonding or deformation degree, which is originated from the attraction between Ti and its neighbor ions. In this paper, we describe the stability with structural parameters of Ti defects of the same type.

The structural parameters of Ti_{Al} type of defects are shown in Fig. 5a. It is clear that the related distances of Ti–NN H in the four situations (Fig. 5a) are almost the same, and much shorter than $d(TiH_2)$, the Ti–H bond length in TiH_2 (about 1.90 Å). This is due to the formation of similar compact TiH_4 complexes in all the Ti substituting Al situations. Accordingly, the contribution of the TiH_4 complex to the deformation and bonding energy is almost the same in these four situations. Hence, the structures outside of the TiH_4 complexes become decisive for the relative stability of the Ti substituting Al defects. Regarding the local structure, Ti_{Al}(1st), which has no NN AlH_4 complexes above Ti (Fig. 3f), is obviously different from the other three situations (*cf.* Fig. 3k, n and p). All the structural parameters show little difference between bulk Ti_{Al}(bulk) and Ti_{Al}(3rd) situation (*cf.* open circles and open squares in Fig. 5a). The corresponding Ti–X (X = H_i, Al_j) distances in the Ti_{Al}(2nd) situation are clearly shorter than those in Ti_{Al}(bulk) and Ti_{Al}(3rd) situations. Especially, the two Ti–Al distances above Ti is very close to $d(TiAl_3)$, the Ti–Al distance in bulk $TiAl_3$ (about 2.72 Å), indicating that Ti has a greater coordination number (CN) in the Ti_{Al}(2nd) situation. The distance of two Ti–Al above Ti is shorter than that of the two under Ti, because the constraint in surface is looser. Obviously, the stability of Ti_{Al}(2nd) is higher than Ti_{Al}(bulk) and Ti_{Al}(3rd) from the structural analysis. As for the Ti_{Al}(1st) situation, although all the corresponding Ti-related bond lengths are very close to those in Ti_{Al}(2nd) situation, the CN of Ti is less due to the surface boundary. In summary, Ti_{Al}(2nd) is obviously the most stable one among the four Ti_{Al} dopants from the structural analysis. Similarly, from the structural analysis, the bonding energy in the Ti_{Na}(1st) situation are more stable than that in the Ti_{Na}(bulk), Ti_{Na}(3rd) and Ti_{Na}(2nd) situation.

The structural parameters of the interstitial type of Ti defects are shown in Fig. 5c, where the situation for the 3rd layer is excluded since there is no remarkable difference found between the 3rd layer and bulk Ti defects in the previous studies. For Ti–X (X = H_i, Al_j) distances of Ti-containing complexes, it is similar to the Ti_{Al} and Ti_{Na} situations that there is little difference between Ti_i(bulk) and Ti_i(2nd). Furthermore, it is shown in Fig. 5c that the distances of Ti–(NN Al) under Ti in the Ti_i(1st) situation is obviously shorter than that in other two situations. As for other Ti–X (X = H_i, Al_j) distances of Ti-containing complexes, their contribution is almost equal to the Ti-binding energy. Consequently, from the structural analysis, Ti_i(1st) is slightly more stable than the other two defects.

$E_d(Ti_M)$, $E_b(Ti_M)$, $H_f(V_M)$ (M = Al, Na, i), as well as $H_f(Ti_M)$ of the three types of extrinsic Ti defects in bulk and

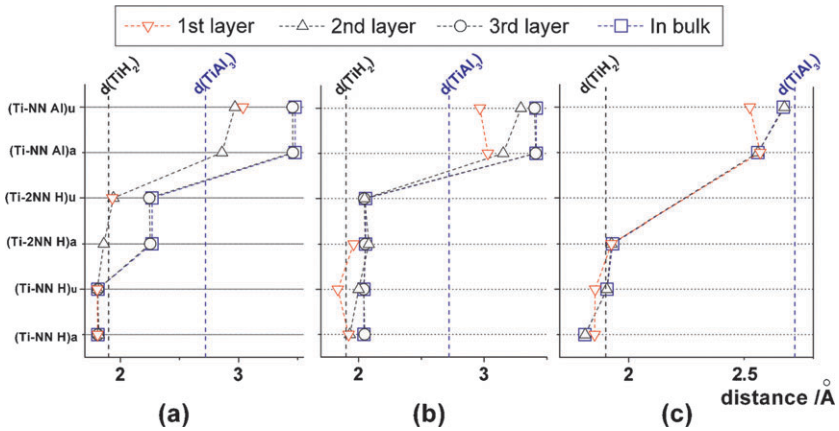

Fig. 5 Structural parameters of local structures of substitutional and single interstitial Ti defects: (a) Ti_{Al} case, (b) Ti_{Na} case, (c) Ti_i case. Subscript "u", "a" represent "under" and "above" respectively.

near surface region of $NaAlH_4$ are shown in Fig. 6. For Ti_{Al} defects in Fig. 6a, $E_b(Ti_M)$ of Ti_{Al}(2nd) is the highest, which is consistent with the shorter Ti-related bonds and higher CN of Ti in the structure (Fig. 5a). When Ti is located at surface, the binding energy of Ti is the lowest, which is mainly due to its low CN. The value of $H_f(V_{Al})$ decreases as the depth of Ti decreases. We know that AlH_4 is a rather stable complex which makes the formation of Al vacancies difficult. The local structures of Al vacancies are shown in Fig. 7 and we can see there are a lot of changes. The high energy "4H local structure" in Ti_{Al}(bulk) situation (Fig. 7a) leads a high vacancy formation enthalpy, while the Al vacancy formation enthalpies near the surface are much lower because of their more stable 2(H–H) local structure (Fig. 7b). The deformation energy in the bulk situation is lower than that near the surface and it is also consistent with analysis of the local structures. The $E_d(Ti_{Al})$ is rather high which is due to large displacement of the NN H/Al ions relative to the Al vacancy local structure. In Ti_{Al}(2nd), Ti_{Al}(3rd) and Ti_{Al}(bulk) situations the Ti-containing complexes are similar, and it is shown in Fig. 6a

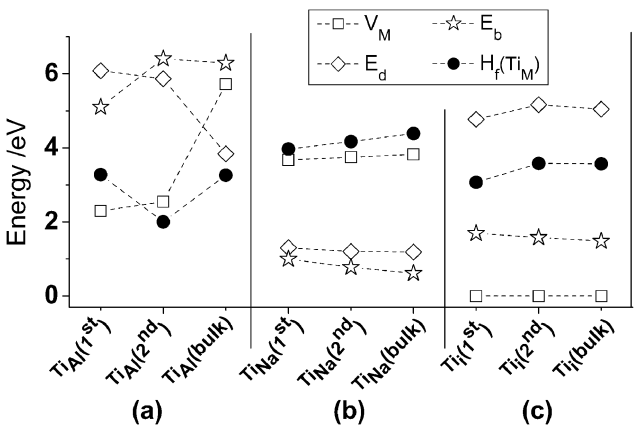

Fig. 6 Deformation energy $E_d(Ti_M)$, binding energy of Ti $E_b(Ti_M)$ and corresponding vacancy formation enthalpies $H_f(V_M)$ (M = Al, Na), (i) of Ti single defects as well as of some combinations in $NaAlH_4$ bulk and near the surface. All the data are given at the hydriding/dehydriding critical point of $NaAlH_4$ and $\mu_{Ti} = -1.59$ eV. V_M (M = i) refers to defect free. (a) Ti_{Al} case, (b) Ti_{Na} case, (c) Ti_i case.

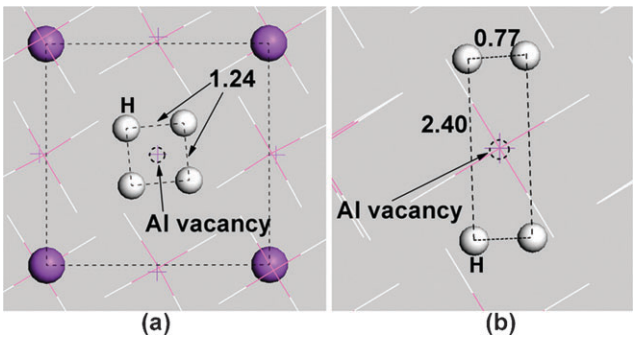

Fig. 7 Local structure of Al vacancy (top view): (a) in $NaAlH_4$ bulk, (b) at the 1st layer of (001) slab. (Unit: Å).

that among these three situations, a higher binding energy corresponds to a higher deformation energy and lower H_f(Ti def).

In the Ti_{Na} case (Fig. 6b) the difference between the values of $H_f(Ti_{Na})$ among the three different defects is not remarkable. We can see that the values of $E_b(Ti_{Na})$ and $E_d(Ti_{Na})$ increase while $H_f(V_{Na})$ decreases with decreasing depth of Ti defects, which is due to a looser constraint on the surface. The changes in $E_b(Ti_{Na})$ and $E_d(Ti_{Na})$ are also consistent with the corresponding structure relaxation. As a result, Ti is favorable at the 1st layer among all the Na vacancies. Just like in Ti_{Al}, Ti_{Na}(2nd), Ti_{Na}(3rd) and Ti_{Na}(bulk) situations, a higher binding energy corresponds to a higher deformation energy and a lower H_f(Ti def).

The energy information for the interstitial type of Ti defects is shown in Fig. 6c. There is little difference in each energy term for the different locations of Ti_i: *viz.* the 2nd layer *vs.* bulk. The binding energy in Ti_i(1st) situation is the greatest while the deformation energy in this situation is the lowest, which seems contradictory at first sight. However, we find in the deformation aspect that the NN Na–Na distance (a parameter for Na–Al octahedron deformation) above Ti in the Ti_i(1st) situation is much longer than the other two situations. Besides, the displacement of Al under Ti is 0.295/0.63/0.63 Å for Ti located at the 1st layer/the 2nd layer/bulk, respectively. This implies that the structural

deformation of Ti_i(1st) is greater than others, but it occurs mainly at the 1st layer which has less constraints. It is understandable that Ti_i(1st) is the most favorable interstitial Ti defect.

From our calculation, the extrinsic Ti defects are favorable to locate at the 1st and 2nd layer, while they are difficult to enter deeper layers. This is consistent with the AES experiment by Gross *et al.*[22] and the EXAFS and XANES experiments by Balde *et al.*[23] It is easy to imagine that Ti accumulates at the shallow surface as its doping amount increases, probably followed by the formation of a Ti-rich interface between $NaAlH_4$ and the Ti-containing substance. We know that the local structure of Ti defects is of a Ti–Al–H complex, which means that there is a competition between the H–Ti phases and Al–Ti phases when the amount of Ti increases. Although the formation ability of $TiAl_3$ phase is the highest[17] under the global thermodynamic equilibrium state under the H-poor hydriding/dehydriding critical point environment, it is difficult to form $TiAl_3$ crystals due to the competition between H–Ti and Al–Ti phases. This could be the reason that amorphous Ti-containing substance is often be found in experiments.[24–26] The Ti-rich layer should be characterized further, because this tight coupling interface probably plays a key role in catalysis of the gas–solid reaction of the Ti–$NaAlH_4$ system.

3.3 Local geometry structure of Ti_{Al}(2nd) and Ti_i(1st) defects

We now compare the local structures around Ti for Ti_{Al}(2nd) and Ti_i(1st) cases in detail (Fig. 8 and 9) which is helpful to reveal the influence of these two Ti defects on the hydriding/dehydriding performance of $NaAlH_4$. There are $TiAl_4H_{20}$ and $TiAl_3H_{12}$ complexes of C_2 symmetry formed around Ti_{Al}(2nd) and Ti_i(1st) situations, respectively. In addition to the Ti–Al–H complexes, neighboring regions of both Ti–Al–H complexes have obvious geometry structure change. Since the influence of Ti on $NaAlH_4$ is a local effect both the complex and its neighbor environment require to be investigated. The comparison in the neighbor region of Ti–Al–H complexes is focused on the NN Na and the 2NN AlH_4 groups of Ti in the 1st layer and we refer it to the "surrounding region" of the Ti-containing complex. The "surrounding region" does not bond with Ti, but deforms when the corresponding Ti defect is introduced.

In the "surrounding region" of Ti-containing complexes (Fig. 8 and 9), the displacements of $Al_{1,2}$ ions and $Na_{1,2}$ ions in

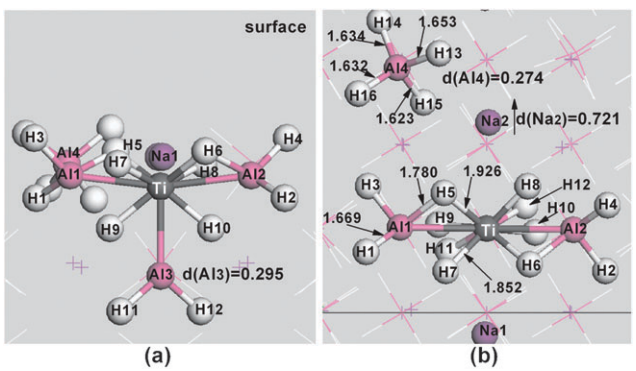

Fig. 8 Relaxed local structures around Ti in the Ti_i(1st) situation: (a) side view; (b) top view.

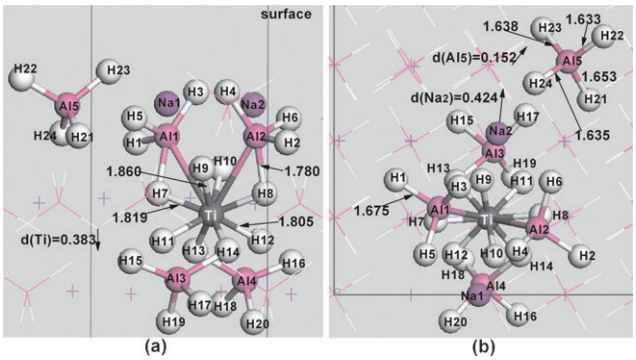

Fig. 9 Relaxed local structures around Ti in the Ti_{Al}(2nd) situation: (a) side view; (b) top view.

Ti_i(1st) situation are larger than that in Ti_{Al}(2nd) situation, especially the Na_1 and Na_2 ions. Besides, a greater displacement of Na corresponds to a greater displacement of Al. This also shows that the 2nd NN AlH_4 groups of Ti (*cf.* Al_4–$H_{13–16}$ in Fig. 8 and Al_5–$H_{21–24}$ in Fig. 9) are also influenced greatly by the Ti defects in both situations, especially for the Ti_i(1st) situation. The deformation of AlH_4 groups in the "surrounding region" is mainly AlH_3–H separation[16] in both situations. Corresponding to a greater displacement of Al_4, the AlH_3–H separation in Ti_i(1st) situation is more significant. The reason for AlH_3–H separation is related to the fact that the AlH_3 is a magic cluster[27] of AlH_x due to its high stability.

The configuration of each Ti-containing complex is more complicated than the related "surrounding region" in both situations. In the Ti_i(1st) situation, the distance between Ti and the three NN AlH_4 groups is very short before relaxation, and the three NN AlH_4 groups are influenced greatly by Ti. After relaxation (Fig. 8), the distances between Ti and the three Al are remarkably shorter than $d(TiAl_3)$, which means that those Ti–Al bonds are very strong. Furthermore, all the three NN AlH_4 groups are destroyed, thus, the deformation of them are not just AlH_3–H separation. The NN H ions of Ti in the three NN AlH_4 groups are captured by Ti, *i.e.* these H ions are bonded with Ti mainly ($H_{7–10}$ in Fig. 8). The 2NN H ions in the three NN AlH_4 groups move close to Ti greatly, and they bond with both Al and Ti, denoted as "bridge H",[12] ($H_{5,6}$ in Fig. 8). The remaining H ions are bonded with Al mainly ($H_{1–4}$ and $H_{11,12}$ in Fig. 8). Consequently, H ions in Ti-containing complexes can be divided into three types based on bonding condition: T_1, H ions bonded with Al mainly; T_2, bridge H; T_3, H ions bonded with Ti mainly. In addition, the deformation in the Ti_i(1st) situation is at the 1st layer mainly.

In the Ti_{Al}(2nd) situation, the distance between Ti and its four NN H ions are very short, as mentioned above, due to a compact TiH_4 form ($H_{9–12}$ in Fig. 9). The distances of Ti–(NN H) in TiH_4 are shorter than the shortest distance of Ti–(NN H) in the $TiAl_3H_{12}$ complex. According to the 18e rule,[13,28] the TiH_4 structure is unstable and Ti needs to attract the four NN AlH_4 groups for a further relaxation. Among the four NN AlH_4 groups, those H ions with shortest distance to Ti move towards the Ti and become "bridge H" ($H_{7,8}$ and $H_{13,14}$ in Fig. 9). Similar to the Ti_i(1st) situation, the deformation of the NN AlH_4 groups of Ti in the Ti_{Al}(2nd) situation are not limited to AlH_3–H separation, while the deformation degree in

this situation is smaller than that in the Ti_i(1st) situation. This is obviously attributed to two facts. The first is that, in the Ti_{Al}(2nd) situation, the distances between Ti and the four AlH_4 groups are greater than that in the Ti_i(1st) situation. The second is that the four AlH_4 groups are partially shielded by a compact TiH_4 unit. As for the Ti–Al bonds in the Ti-containing complexes, all the distances in the $TiAl_4H_{20}$ complex are longer than that in the $TiAl_3H_{12}$ complex. Meanwhile, the deformation for the four NN H ions of Ti is substantial in the Ti_{Al}(2nd) situation, which is in line with the compact TiH_4 structure. Therefore, the deformation in the $TiAl_4H_{20}$ complex is mainly in the short-range of Ti, and deformation degree in the region out of TiH_4 in the $TiAl_4H_{20}$ complex is smaller than that in the $TiAl_3H_{12}$ complex. According to the opinion mentioned above that high attraction of Ti leads to high deformation, the coupling degree in the $TiAl_3H_{12}$ complex is higher than that in the region outside of TiH_4 in the $TiAl_4H_{20}$ complex.

3.4 Influence of the two stable Ti defects on the decomposition of $NaAlH_4$

The hydrogen release ability is often characterized by $H_f(V_H)$.[29] Later, Liu *et al.*[12] adopted $H_f(V_{H-H})$ as another criterion. Furthermore, Fu *et al.*[30] reported that $(AlH_3)_n$ is released during the hydriding/dehydriding of $NaAlH_4$. Gunaydin *et al.*[16] also pointed out that the AlH_3 vacancy plays an important role on the decomposition of $NaAlH_4$. In addition, Araujo[29] reported that Na vacancy can promote the decomposition of $NaAlH_4$. Here, we adopt all of $H_f(V_H)$, $H_f(V_{H-H})$, $H_f(V_{AlH_3})$ and $H_f(V_{Na})$ as the score card of the influence of the extrinsic Ti defects on $NaAlH_4$ decomposition. The formation enthalpies of these four vacancies are symbolized as H_f(vacancy) later. Generally, there are quite a few configurations for each type of complex vacancy due to the complicated local structure around Ti. The configuration with *minimum* formation enthalpy at the hydriding/dehydriding critical point is a natural choice for each type of vacancies and they are listed in Table 1 and Table 2 and illustrated in Fig. 10.

We can see that the formation energies of all the four vacancies are lower when Ti is introduced, which means that the Ti dopants play a critical role on promoting the decomposition of $NaAlH_4$. Since the configurations within Ti–Al–H complexes are more complicated than the "surrounding region", here we discuss the vacancies in "surrounding region" firstly.

From Tables 1 and 2 and Fig. 10, we conclude that:

(i) All the $H_f(V_{Na})$ decrease significantly when extrinsic Ti defects are introduced, especially in the Ti_i(1st) situation. An important reason for the reduction of $H_f(V_{Na})$ around Ti defects is that Na ions are pushed away significantly by the Ti defect in the "surrounding region" of $TiAl_4H_{20}$ and $TiAl_3H_{12}$ complexes, which can be seen from the geometric structure, and the displacement of Na in the latter situation is noticeably greater. The activity of Na increases when Na atom deviates from the original equilibrium site, which makes $H_f(V_{Na})$ decrease. Therefore, $H_f(V_{Na})$ in Ti_i(1st) situation is smaller than that in the Ti_{Al}(2nd) situation because of the greater displacement of Na in the former situation.

(ii) Both $H_f(V_{AlH_3})$ and $H_f(V_H)$ decrease in the "surrounding region" of the two Ti–Al–H complexes, especially in the Ti_i(1st) situation. From the structure aspect, the AlH_4 complex in the clean (001) slab transforms to an AlH_3–H structure when Ti is introduced. As a result, the AlH_4 complex is easy to break into two units: H and AlH_3. Therefore both $H_f(V_{AlH_3})$ and $H_f(V_H)$ corresponding to the AlH_3–H configuration are lower than that in AlH_4 of the clean slab. The displacement of Al_4 in Ti_i(1st) case is greater than that of Al_5 in the Ti_{Al}(2nd) case. Accordingly, the separation of AlH_3–H in the Ti_i(1st) case is more marked. It is the main reason that both $H_f(V_{AlH_3})$ and $H_f(V_H)$ in Ti_i(1st) case are lower than that in the Ti_{Al}(2nd) situation. This is consistent with Gunaydin's proposal[16] that Ti plays a role in the catalytic breaking of AlH_3–H bonds.

Now we compare vacancies within the two Ti–Al–H complexes with a focus on $H_f(V_H)$. At first, the $H_f(V_H)$ of type T_1 H ions in the $TiAl_4H_{20}$ complex is lower than that in the $TiAl_3H_{12}$ complex, because the corresponding Al–H bond length in $TiAl_4H_{20}$ complex is longer (1.676 *vs.* 1.669 Å). Similarly, the $H_f(V_H)$ for H of type T_3 in the $TiAl_4H_{20}$ complex is lower than that in the $TiAl_3H_{12}$ complex, which is reflected by the relation of their Ti–H bond lengths (1.860 *vs.* 1.852 Å). The $H_f(V_H)$ for H of type T_1 is lower than that of type T_3 in both Ti-containing complexes, because the affinity of Ti–H is stronger than that of Al–H. Furthermore, it is shown that the bridge H (T_2) has a greater $H_f(V_H)$ than H of types T_1 and T_3 in both Ti-containing complexes, and $H_f(V_H)$ of T_2 type H in the $TiAl_3H_{12}$ complex is higher than that in the $TiAl_4H_{20}$ complex. Regarding the structural parameters, the Al–H/Ti–H distance corresponding to T_2 type of H is 1.78/1.819 Å and 1.78/1.926 Å in $TiAl_4H_{20}$ and $TiAl_3H_{12}$, respectively, which means that the latter has a longer bond length but a greater $H_f(V_H)$. In addition, it is shown that the $H_f(V_H)$ for the three types of H in both situations with the Ti defects are lower than that in the clean (001) slab, which is consistent with

Table 1 The vacancy formation enthalpies around Ti_{Al}(2nd) defect and a clean (001) slab (*cf.* Fig. 9 and 3s) (unit: eV)

Vacancy	$H(T_1)$	$H(T_2)$	$H(T_3)$	H–H	AlH_3	Na
Configuration of defect (in complex)	H_1,H_2[a]	H_7,H_8	H_9,H_{10}	H_3 & H_4[b]	Al_2 & H_2 & H_4 & H_6	
H_f(vacancy)	−0.25	0.39	0.25	0.30	0.34	
Configuration of defect (surrounding region)	H_{21}			H_{21} & H_{23}	Al_5 & H_{22} & H_{23} & H_{24}	Na_1
H_f(vacancy)	1.29			1.15	0.56	0.81
In clean (001) slab	H_1			H_1 & H_2	Al_1 & H_1 & H_2 & H_3	Na
H_f(vacancy)	1.51			1.07	0.64	3.63

[a] Symbol "," means "logic or". [b] Symbol "&" means "logic and".

Table 2 The vacancy formation enthalpies around Ti_i(1st) defect (Fig. 8) (unit: eV)

Vacancy	$H(T_1)$	$H(T_2)$	$H(T_3)$	H–H	AlH_3	Na
Configuration of defect (in complex)	H_1,H_2	H_5,H_6	H_7,H_8	H_{11} & H_{12}	Al_2 & H_2 & H_4 & H_6	
H_f(vacancy)	0.33	0.66	0.50	0.44	0.50	
Configuration of defect (surrounding region)	H_{13}			H_{13} & H_{15}	Al_4 & H_{14} & H_{15} & H_{16}	Na_1
H_f(vacancy)	1.16			0.52	0.23	0.40

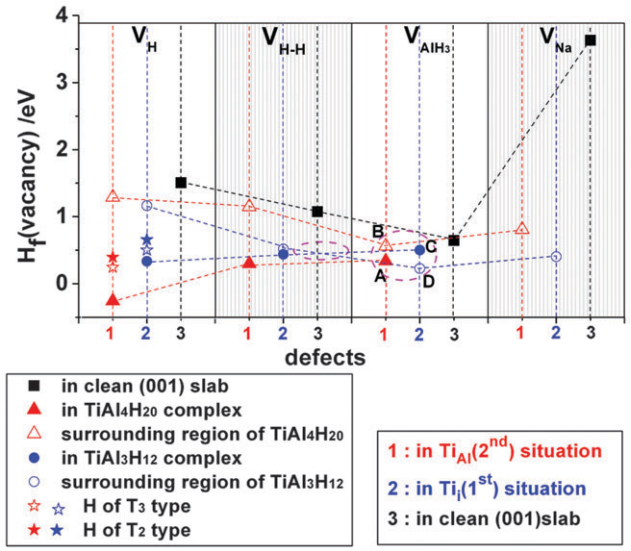

Fig. 10 $H_f(V_H)$, $H_f(V_{H-H})$, $H_f(V_{AlH_3})$ and $H_f(V_{Na})$ in $TiAl_4H_{20}$ and $TiAl_3H_{12}$ complexes and "surrounding region" of these two complexes. Corresponding data for a clean (001) slab are also plotted for the reference.

conclusions from earlier reports[9–11] that the formation of Ti–Al can weaken Al–H bonds. The results are not straightforward. We can see that a stronger Ti–Al bond in $TiAl_3H_{12}$ complex does not correspond to a lower $H_f(V_H)$, but actually higher than that in $TiAl_4H_{20}$ complex. Liu *et al.*[13] considered that the $TMAl_3H_{12}$ (TM = Sc–Co) complexes follow the 18-electron rule[28] whereas the $TiAl_3H_{12}$ complex is a 2e electron-deficient complex. If the $TiAl_4H_{20}$ complex also obeys the 18-electron rule, it is a one-electron-rich complex which is in line with its low $H_f(V_H)$ of H_1/H_2 (Fig. 10). Furthermore, it was reported that the electronic population on the Al–H bond is 0.88 and clearly the covalent bond dominates the interaction between H and Al.[5] There are also hybridization between Al and Ti in Ti_{Al}.[9] Those results indicate that the interaction between Ti and Al is also dominated by the covalent bond. Owing to the saturation property of the covalent bond, it is expected that the bond strength of Ti–H and Ti–Al would decrease when the CN of Ti increases to some extent, consistent with that reported by Vajeeston *et al.*[31] We know that the CN of Ti in the electron-rich $TiAl_4H_{20}$ complex are higher than that in the $TiAl_3H_{12}$ complex, which is an important reason for the lower $H_f(V_H)$ in the $TiAl_4H_{20}$ complex.

After the comparison of vacancy formation energies between the two Ti–Al–H complexes, it is necessary to make a comparison between the "surrounding regions" and the complexes themselves. It is easy to see from Fig. 10 that H_f(vacancy) values in the $TiAl_3H_{12}$ complex are lower than that in its "surrounding region", except for $H_f(V_{AlH_3})$ of the $TiAl_3H_{12}$ complex possibly due to the weakened Al–H bond strength by the formation of Al–Ti bonds. On the other hand, in the "surrounding region" all the related H_f(vacancy) are higher than those in $TiAl_4H_{20}$ complex. In addition, there is another reason that the deformation in the "surrounding region" is obviously smaller than that within the complex in Ti_{Al}(2nd) situation.

Generally, the H–H and AlH_3 complex vacancies are more complicated than single vacancies, because it involves combination of some single vacancies. We found that the lowest $H_f(V_{H-H})$ correspond to two H of type T_1 with short distance. As for $H_f(V_{AlH_3})$, it leads to a "crossover" in Fig. 10 (marked by ellipses). According to Tables 1 and 2 and Fig. 10, the value of $H_f(V_{AlH_3})$ in those situations (labeled as A, B, C and D) can be sequenced from low to high as D < A < C < B. On the other hand, the distance between Ti and its neighbor AlH_4 groups before structure relaxation can be arranged from short to long as C < A < D < B, which is corresponding to the sequence of the strong to weak interactions. $H_f(V_{AlH_3})$ in these situations are expected to follow the order of C < A < D < B if a stronger Ti–AlH_4 interaction aids the release of AlH_3. However, the calculated $H_f(V_{AlH_3})$ is ordered as D < A < C < B. It can be speculated that the influence on $H_f(V_{AlH_3})$ by the interaction between Ti and neighboring AlH_4 is not monotonic. After making a comparison of local structures, we found that in situations B and D, the deformation of the 2NN AlH_4 is mainly AlH_3–H separation, and thus, the larger deformation the lower is $H_f(V_{AlH_3})$. In the A and C situations, the interaction between Ti and its NN AlH_4 is too strong to limit deformation merely in AlH_3–H separation. Especially, the structure of the 2NN AlH_4 groups is influenced greatly in case C. It is expected that the complicated bonding hinders the release of AlH_3 in case C. As a result, $H_f(V_{AlH_3})$ in case C turns to be higher than that in cases D and A. Therefore, an optimal interaction strength between Ti and the AlH_4 group is expected to minimize $H_f(V_{AlH_3})$, which may be applied to the situation of other transition metal defects in $NaAlH_4$.

As shown in Fig. 10, in the Ti_i(1st) situation, the lowest vacancy formation enthalpy is $H_f(V_{AlH_3})$, which characterizes the influence of Ti_i(1st) on the decomposition of $NaAlH_4$. In the Ti_{Al}(2nd) situation, the lowest vacancy formation enthalpy is $H_f(V_H)$, but it is not suitable for describing the H_2 release ability in this situation. This is because H_2 is always released after H–H is formed at a small local region of $NaAlH_4$ matrix, but not assembled by two free H atoms escaping from the $NaAlH_4$ matrix. Therefore, the hydrogen release ability should be described with $H_f(V_{AlH_3})$ and $H_f(V_{H-H})$ in Ti_{Al}(2nd)

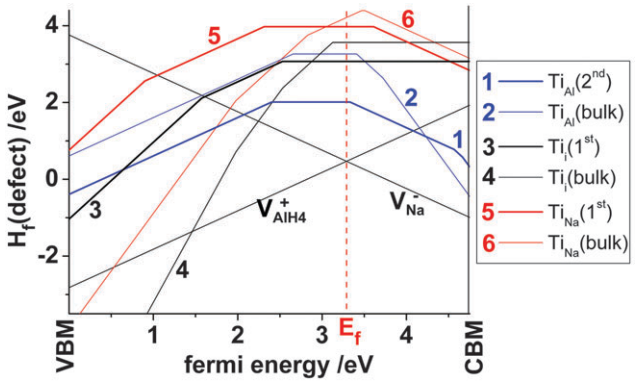

Fig. 11 The relation of charged defect formation enthalpies of the extrinsic Ti defects and Fermi energy under the chemical environment of the hydriding/dehydriding critical point and $\Delta\mu_{Ti} = -1.59$ eV.

situation. Generally, the low $H_f(V_{AlH_3})$ in these two situations are consistent with the AlH_3 mechanism of $NaAlH_4$.[16,30,32] Therefore, it is a key factor for the dehydriding of $NaAlH_4$ to lower the value of $H_f(V_{AlH_3})$. On the other hand, it also implies that increasing the formation ability of AlH_3 as well as the interaction energy between the $(AlH_3)_n$ molecules and Ti defects will promote rehydriding ability of $NaAlH_4$.[33]

4. Charged Ti defects in bulk and surface range

Now we consider the stable charge state of the extrinsic Ti defects by calculating the H_f(def) of charged Ti_i(bulk), Ti_{Al}(bulk) and Ti_{Na}(bulk) as well as Ti_i(1st), Ti_{Al}(2nd) and Ti_{Na}(1st). Five oxidation states of Ti (Ti^0, Ti^{1+}, Ti^{2+}, Ti^{3+} and Ti^{4+}) are taken into account. The charged defect formation enthalpies are calculated by eqn (3):[21]

$$H_f^{D,q}(E_F,\mu) = E^{D,q} - E(\text{bulk/slab}) + \sum_i n_i\mu_i + q[E_v(\text{bulk/slab}) + E_F] \quad (3)$$

Here, $E^{D,q}/E$ are total energy with/without defect respectively; E_v(bulk/slab) is the energy at the valence band maximum (VBM) in bulk/slab without defects. Our calculated value, 4.75 eV, is adopted here for the band gap of $NaAlH_4$, since we cannot find any experimental value. Here the image charge correction[34] (typically within 200 m eV) is not employed, which is not expected to affect our conclusion here. The change of the defect formation enthalpies of the above mentioned six Ti defects with respect with the Fermi level is shown in Fig. 11.

The Fermi level of $NaAlH_4$ is pinned by V^-_{Na} and $V^+_{AlH_4}$ in the undoped $NaAlH_4$ according to the overall charge neutrality, which is around 3.30 eV above the VBM of bulk $NaAlH_4$.[32] It is shown in Fig. 11 that the Fermi level is still pinned by the intrinsic vacancies of V^-_{Na} and $V^+_{AlH_4}$ when extrinsic Ti defects are introduced. We find that, even in the situation of Ti-richest condition (*i.e.* $\Delta\mu_{Ti} = 0$ eV), Ti dopant has little influence on the equilibrium Fermi level (a global parameter) of $NaAlH_4$. Although the total concentration of Ti defects is much lower than those of V^-_{Na} and $V^+_{AlH_4}$, their influence on the surface region could be remarkable since they are accumulated at the surface region.

When the Ti defects are located in the bulk of $NaAlH_4$, Ti_{Al}(bulk), Ti_i(bulk) and Ti_{Na}(bulk) exist in 0, 0 and +1 charged states, respectively, at the equilibrium Fermi level. The difference between $H_f(Ti^+_{Na}(\text{bulk}))$ and $H_f(Ti^0_{Na}(\text{bulk}))$ is small, because the transition state of Ti^+_{Na}(bulk)/Ti^0_{Na}(bulk) are close to the pinned Fermi level. Hence, the order of the defect formation enthalpies is not changed with the consideration of stable charge state, *i.e.*, $(H_f(Ti^0_{Al}(\text{bulk})) < H_f(Ti^0_i(\text{bulk})) < H_f(Ti^+_{Na}(\text{bulk}))$. The Ti_i(1st), Ti_{Al}(2nd) and Ti_{Na}(1st) are all neutral at the pinned Fermi level. Therefore, our earlier discussion on the energetics and structure of extrinsic defects based on the neutral charge state is still valid.

5. Conclusion

The extrinsic Ti defects of $NaAlH_4$ have been systematically studied using the DFT method with plane-wave basis set and PAW potentials under the hydriding/dehydriding critical point environment. The following conclusion can be made:

(1) Ti_{Al}(2nd) is the most favorable single Ti defect in $NaAlH_4$, while Ti_i(1st) is the second favorable one and dominates in the 1st layer of the (001) slab. All the H_f(vacancy) in both Ti_{Al}(2nd) and Ti_i(1st) situations are lower than the corresponding H_f(vacancy) in a clean (001) slab of $NaAlH_4$, and thus Ti promotes the decomposition of $NaAlH_4$.

(2) In the "surrounding region" of complexes, all the H_f(vacancy) in Ti_i(1st) situations are higher than that in Ti_{Al}(2nd) complex, while within the Ti-containing complex all the H_f(vacancy) in Ti_i(1st) situations are lower than those in the Ti_{Al}(2nd) situations. This is due to a greater deformation in the "surrounding region" as well as a stronger coupling inside the $TiAl_3H_{12}$ complex with respect to the $TiAl_4H_{20}$ complex.

(3) $H_f(V_{AlH_3})$ can characterize the hydrogen release ability of $NaAlH_4$ in both Ti_{Al}(2nd) and Ti_i(1st) complexes, and $H_f(V_{H-H})$ in Ti_{Al}(2nd) situation is also a good choice for the scorecard of the hydrogen release ability of $NaAlH_4$.

Acknowledgements

This work was financially supported by the NSFC under project No. 50631020, MOST under project 2010CB631302, and the Fundamental Research Funds for the Central Universities, SCUT, under project 2009ZZ0068. Computing resources from the High Performance Grid Computer Center of South China University of Technology (SCUTGrid) are also gratefully acknowledged.

References

1 B. Bogdanovic and M. Schwickardi, *J. Alloys Compd.*, 1997, **253–254**, 1–9.
2 P. Chen, Z. Xiong, J. Luo, J. Lin and K. L. Tan, *Nature*, 2002, **420**, 302–304.
3 Y. Nakamori, K. Miwa, A. Ninomiya, H. Li, N. Ohba, S.-i. Towata, A. Zuttel and S.-i. Orimo, *Phys. Rev. B: Condens. Matter Mater. Phys.*, 2006, **74**, 045126–045129.
4 K. Chlopek, C. Frommen, A. Leon, O. Zabara and M. Fichtner, *J. Mater. Sci.*, 2007, **17**, 3496–3503.

5 X. Ke and I. Tanaka, *Phys. Rev. B: Condens. Matter Mater. Phys.*, 2005, **71**, 024117–024116.
6 J. Íñiguez, T. Yildirim, T. J. Udovic, M. Sulic and C. M. Jensen, *Phys. Rev. B: Condens. Matter Mater. Phys.*, 2004, **70**, 060101.
7 J. Íñiguez and T. Yildirim, *Appl. Phys. Lett.*, 2005, **86**, 103109–103103.
8 O. M. Løvvik and S. M. Opalka, *Phys. Rev. B: Condens. Matter Mater. Phys.*, 2005, **71**, 054103.
9 K. Bai and P. Wu, *Appl. Phys. Lett.*, 2006, **89**, 201904–201903.
10 A. Blomqvist, C. M. Araujo, P. Jena and R. Ahuja, *Appl. Phys. Lett.*, 2007, **90**, 141904–141903.
11 J. J. Liu and Q. F. Ge, *Chem. Commun.*, 2006, 1822–1824.
12 J. J. Liu and Q. F. Ge, *J. Phys. Chem. B*, 2006, **110**, 25863–25868.
13 J. J. Liu, Y. Han and Q. F. Ge, *Chem.–Eur. J.*, 2009, **15**, 1685–1695.
14 A. Marashdeh, R. A. Olsen, O. M. Lovvik and G.-J. Kroes, *J. Phys. Chem. C*, 2007, **111**, 8206–8213.
15 T. Vegge, *Phys. Chem. Chem. Phys.*, 2006, **8**, 4853–4861.
16 H. Gunaydin, K. N. Houk and V. Ozolins, *Proc. Natl. Acad. Sci. U. S. A.*, 2008, **105**, 3673–3677.
17 C. K. Huang, Y. J. Zhao, T. Sun, J. Guo, L. X. Sun and M. Zhu, *J. Phys. Chem. C*, 2009, **113**, 9936–9943.
18 G. Kresse and J. Furthmuller, *Comput. Mater. Sci.*, 1996, **6**, 15–50.
19 G. Kresse and D. Joubert, *Phys. Rev. B: Condens. Matter Mater. Phys.*, 1999, **59**, 1758.
20 J. P. Perdew, J. A. Chevary, S. H. Vosko, K. A. Jackson, M. R. Pederson, D. J. Singh and C. Fiolhais, *Phys. Rev. B: Condens. Matter*, 1992, **46**, 6671.
21 S. B. Zhang and J. E. Northrup, *Phys. Rev. Lett.*, 1991, **67**, 2339.
22 K. J. Gross, S. Guthrie, S. Takara and G. Thomas, *J. Alloys Compd.*, 2000, **297**, 270–281.
23 C. P. Balde, H. A. Stil, A. M. J. van der Eerden, K. P. deJong and J. H. Bitter, *J. Phys. Chem. C*, 2007, **111**, 2797–2802.
24 J. Graetz, J. J. Reilly, J. Johnson, A. Y. Ignatov and T. A. Tyson, *Appl. Phys. Lett.*, 2004, **85**, 500–502.
25 C. M. Andrei, J. C. Walmsley, H. W. Brinks, R. Holmestad, S. S. Srinivasan, C. M. Jensen and B. C. Hauback, *Appl. Phys. A: Mater. Sci. Process.*, 2005, **80**, 709–715.
26 Viktor P. Balema and L. Balema, *Phys. Chem. Chem. Phys.*, 2005, **7**, 1310–1314.
27 B. K. Rao, P. Jena, S. Burkart, G. Ganteför and G. Seifert, *Phys. Rev. Lett.*, 2001, **86**, 692.
28 D. M. P. Mingos, *J. Organomet. Chem.*, 2004, **689**, 4420–4436.
29 C. M. Araújo, S. Li, R. Ahuja and P. Jena, *Phys. Rev. B: Condens. Matter Mater. Phys.*, 2005, **72**, 165101.
30 Q. J. Fu, A. J. Ramirez-Cuesta and S. C. Tsang, *J. Phys. Chem. B*, 2006, **110**, 711–715.
31 P. Vajeeston, P. Ravindran, R. Vidya, H. Fjellvag and A. Kjekshus, *Appl. Phys. Lett.*, 2003, **82**, 2257–2259.
32 C. K. Huang, Y. J. Zhao, J. Guo and M. Zhu, unpublished work.
33 S. Chaudhuri and J. T. Muckerman, *J. Phys. Chem. B*, 2005, **109**, 6952–6957.
34 G. Makov and M. C. Payne, *Phys. Rev. B: Condens. Matter*, 1995, **51**, 4014.

